Catal Lett (2008) 122:188–195
DOI 10.1007/s10562-007-9368-2

EXAFS Study on Structural Change of Charcoal-supported Ruthenium Catalysts during Lignin Gasification in Supercritical Water

Aritomo Yamaguchi · Norihito Hiyoshi · Osamu Sato · Mitsumasa Osada · Masayuki Shirai

Received: 5 September 2007 / Accepted: 23 November 2007 / Published online: 12 December 2007

Abstract Lignin gasification in supercritical water over charcoal supported ruthenium trivalent salts was studied using a batch reactor at 673 K. Ruthenium (III) nitrosyl nitrate on charcoal ($Ru(NO)(NO_3)_3$/C) was more active than ruthenium (III) chloride on charcoal ($RuCl_3$/C) for the gasification reaction. EXAFS analysis revealed that ruthenium metal particles were formed in both $RuCl_3$/C and $Ru(NO)(NO_3)_3$/C catalysts during the lignin gasification and that the size of ruthenium metal in $Ru(NO)(NO_3)_3$/C was smaller than that in $RuCl_3$/C. It was concluded that well-dispersed ruthenium metal particles were active for the lignin gasification in supercritical water.

Keywords Lignin gasification · Supercritical water · Supported ruthenium catalyst · EXAFS · Metal particle

1 Introduction

Utilization of lignin has attracted much attention as renewable energy source because the green house effect of carbon dioxide released from the combustion of fossil fuel has to be reduced to control the global warming [1]. The gasification of lignin is needed for its efficient use as a high quality energy source for fuel cell or as liquid fuel by Fisher-Tropsch reaction. Supercritical water ($T_c = 647.3$ K, $P_c = 22.1$ MPa) gasification is a promising technique to reduce the lignin gasification temperature [2–4]. We have reported that lignin was converted to alkylphenol and formaldehyde via hydrolysis in supercritical water and then alkylphenol and formaldehyde decomposed to gaseous products over metal catalysts [5–9]. We have also reported that titania or charcoal supported ruthenium metal catalysts were effective for the lignin gasification in supercritical water at 673 K [7]. Park and Tomiyasu reported that ruthenium oxide (RuO_2) was active for lignin gasification in supercritical water at 723 K and proposed the reaction mechanism that lignin was partially oxidized by RuO_2 and ruthenium (IV) was reduced to ruthenium (II) during the gasification [10, 11]. They also claimed that the ruthenium (II) was reoxidized by water to form ruthenium (IV) and hydrogen, indicating that the lignin gasification proceeds due to the catalytic redox couple formed between ruthenium (IV) and ruthenium (II) species.

In this manuscript, we describe the structural change of ruthenium (III) species and propose the reaction mechanism of lignin gasification over supported ruthenium (III) salt catalysts. We also report the catalytic performance of charcoal-supported ruthenium (III) salts for the gasification in supercritical water at 673 K. We observed that the ruthenium (III) species in the supported ruthenium salts were reduced to ruthenium metal particles, which were responsible for the lignin gasification activities in supercritical water.

2 Experimental

2.1 Catalyst Preparation

Lignin (organosolv-lignin powder) was purchased from Aldrich and used without further purification. Its molecular

A. Yamaguchi · N. Hiyoshi · O. Sato · M. Shirai (✉)
Research Center for Compact Chemical Process, National Institute of Advanced Industrial Science and Technology (AIST), 4-2-1 Nigatake, Miyaginoku, Sendai 983-8551, Japan
e-mail: m.shirai@aist.go.jp

M. Osada
Department of Chemical Engineering, Ichinoseki National College of Technology, Takanashi, Hagisho, Ichinoseki, Iwate 021-8511, Japan

formula was $C_{42.39}H_{45.46}O_{12.15}$, as determined by an ultimate CHNS analyzer (Perkin-Elmer, model 2400) [12]. A model compound of alkylphenol, 4-propylphenol was purchased from Tokyo Chemical Industry. The catalysts used were prepared by an impregnation method using activated charcoal powder (Wako Pure Chemical Industries) and an aqueous solution of ruthenium (III) chloride hydrate (Wako Pure Chemical Industries) or ruthenium (III) nitrosyl nitrate solution in dilute nitric acid (Aldrich) as follows. The aqueous solution of ruthenium precursor and charcoal powder were stirred for 1 h at ambient temperature and evaporated to dryness at 323 K under reduced pressure by a rotary evaporator. Then the samples were dried for 10 h at 373 K in an oven, which were represented as $RuCl_3$/C and $Ru(NO)(NO_3)_3$/C hereinafter, based on the corresponding ruthenium precursors used. A charcoal-supported ruthenium (Ru/C) catalyst was purchased from Wako Pure Chemical Industries and used as a reference catalyst. The amount of ruthenium in all the catalysts was regulated to be 5 wt%.

2.2 Gasification

Gasification of lignin was carried out in a SUS 316 tube, of which inner volume is 6.0 cm^3. The catalyst (0.15 g), lignin (0.10 g), and water (3.0 g) were loaded in the tube and gas in the reactor was purged with argon gas. The reactor was submerged into a sand bath (Takahashi Rica, model TK-3) at 673 K for a given reaction time. The partial pressure of water was 37.1 MPa in the supercritical phase at 673 K and 0.5 g cm^{-3} (density) of water [13]. After the reaction, the tube was submerged into a water bath for cooling to ambient temperature. Gaseous products were analyzed by a gas chromatography (Shimadzu, GC-8A) using a Shincarbon ST column and a thermal conductivity detector. Liquid and solid products in the tube were recovered with water and filtered to separate water-insoluble fraction from water-soluble fraction. Amounts of organic carbon and ruthenium species in the water-soluble fraction were evaluated using a total organic carbon analyzer (Shimadzu, TOC-V_{CSN}) and an inductively coupled plasma emission spectrometry (Seiko, ICP-SPS 1500R), respectively. The water-insoluble fraction was washed with tetrahydrofuran (THF, Wako Pure Chemical Industries) and filtered to separate THF-insoluble solid fraction from THF-soluble fraction. Amount of THF-insoluble product (char) was estimated by subtracting the weight of the catalyst loaded from the amount of THF-insoluble solid fraction.

A product yield based on carbon and gas composition are defined as given below,

$$\text{Product yield based on carbon(C\%)} = \frac{\text{mol of carbon atom in product}}{\text{mol of carbon atom in lignin loaded}} \times 100 \quad (1)$$

$$\text{Gas composition(\%)} = \frac{\text{mol of gas product}}{\text{sum of mol of gas product}} \times 100 \quad (2)$$

2.3 Characterization

X-ray diffraction (XRD) patterns of the catalysts before and after the gasification were recorded using a Rigaku RINT 2200VK/PC with Cu Kα radiation under air-exposed condition. Extended X-ray absorption fine structure (EXAFS) measurement was performed using a synchrotron radiation ring at AR-NW10A, Photon Factory, KEK with a Si (311) double-crystal monochrometer in transmission mode. The catalyst samples were recovered from the SUS reactors quickly and filled into EXAFS cells as water suspension. The EXAFS spectra of the catalysts, which were exposed to air, were measured at room temperature. The spectra were analyzed by a UWXAFS package [14]. After background subtraction, a k^3-weighted EXAFS function in the k range of 30–140 nm^{-1} was Fourier transformed into an R-space. The spectrum was fitted in the corresponding k-space of the R range 0.10–0.30 nm. The Fourier transforms were fitted using the first shell of Ru–Ru. The backscattering amplitudes and phase shifts were calculated by the FEFF8 code [15]. The coefficient of effective amplitude reduction factor (s_0^2) of Ru–Ru bond was estimated from the fitting result of a standard sample of ruthenium metal powder. The fitting parameters were coordination number (CN), interatomic distance (R), Debye-Waller factor (σ^2), and a correction of the threshold energy (ΔE_0).

2.4 Results and Discussion

Table 1 shows the product yields and gas composition of lignin gasification at 673 K for 1 h in supercritical water over the ruthenium-based catalysts and the charcoal sample without ruthenium species. The $RuCl_3$/C and $Ru(NO)(NO_3)_3$/C catalysts, which were not reduced during the preparation, as well as the reduced Ru/C catalyst showed lignin gasification activities. $Ru(NO)(NO_3)_3$/C was almost as active as Ru/C for the gasification; however, the $RuCl_3$/C catalyst was three times less active than those catalysts, as revealed by their gas yields in Table 1.

Table 1 Product yield, gasification rate, and composition of catalytic lignin gasification in supercritical water[a]

Catalyst	Gas yield (C%)	Gasification rate[c] (10^{-6} C-mol cat-g^{-1} s^{-1})	Gas composition (%)					Water soluble (C%)	THF soluble[b] (C%)	THF insoluble (C%)
			H_2	CO	CH_4	CO_2	C_2–C_4 gases			
Charcoal	8.4	1.8	6.9	23.6	15.4	52.8	1.4	10.9	42.3	38.4
$RuCl_3$/C	24.3	5.6	14.6	0.0	17.1	65.7	2.6	7.1	39.2	29.4
$Ru(NO)(NO_3)_3$/C	75.4	14.2	3.1	2.8	41.9	51.4	0.9	1.0	19.4	4.2
Ru/C	87.5	15.7	3.1	0.7	47.4	48.2	0.6	0.1	9.4	3.0

[a] Reaction condition; lignin 0.10 g, catalyst 0.15 g, water density 0.50 g cm^{-3}, 673 K, 1 h

[b] THF soluble (C%) was calculated to be 100−(gas yield (C%))−(water soluble (C%))−(THF insoluble (C%))

[c] Gasification rate was calculated from initial gas yield

Figure 1 shows the gas yields and composition of lignin gasification in supercritical water as a function of reaction time. Lignin in the reactor was almost completely gasified over the $Ru(NO)(NO_3)_3$/C and Ru/C catalysts in supercritical water at 673 K for 3 h; however, lignin gasification over the $RuCl_3$/C catalyst reached a plateau at about 30 C% lignin conversion after 1 h (Fig. 1a). The percentage of hydrogen in the gaseous products over $Ru(NO)(NO_3)_3$/C and Ru/C was *ca.* 10% at 20 min and decreased to *ca.* 3% after 1 h (Fig. 1c, d). In contrast to this, the percentage of methane over the $Ru(NO)(NO_3)_3$/C and Ru/C catalysts increased with increase in reaction time from 20 min to 1 h. These results are in accordance with the earlier report that carbon dioxide and hydrogen were formed at an early stage of lignin gasification, which further reacted to produce methane [16]. The hydrogen and carbon dioxide composition of the gaseous products over the $RuCl_3$/C catalyst was higher than those over the other

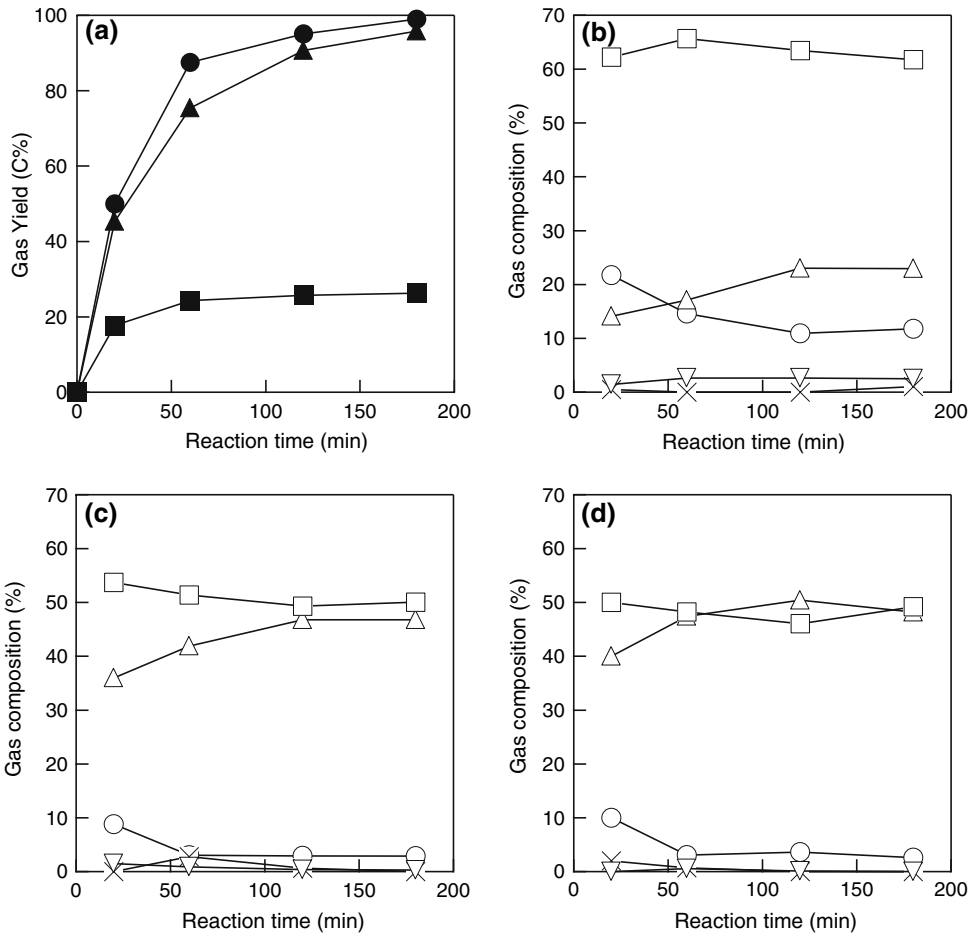

Fig. 1 Carbon yield and gas composition for lignin gasification in supercritical water at 673 K and 0.5 g cm^{-3} of water density: (**a**) gas yield (catalyst; $RuCl_3$/C (■), $Ru(NO)(NO_3)_3$/C (▲), and Ru/C (●)), gas composition over $RuCl_3$/C (**b**), $Ru(NO)(NO_3)_3$/C (**c**), and Ru/C (**d**) (H_2 (◯), CH_4 (△), CO (×), CO_2 (□), and C_2–C_4 gases (▽))

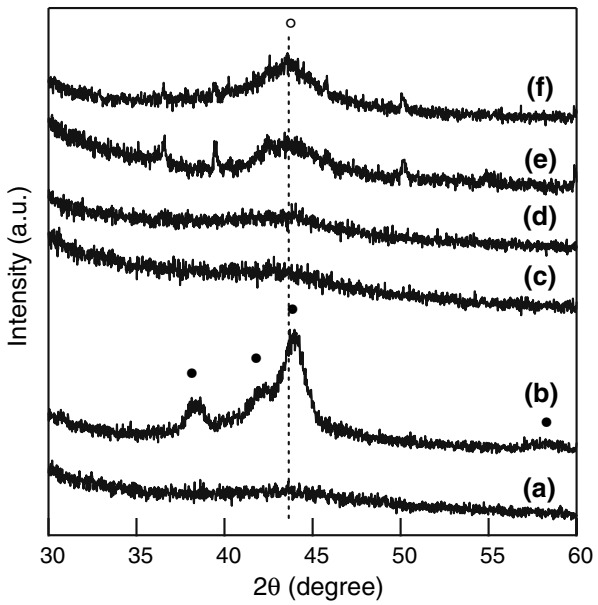

Fig. 2 XRD patterns for $RuCl_3$/C, $Ru(NO)(NO_3)_3$/C, and Ru/C before and after the lignin gasification in supercritical water at 673 K for 1 h. $RuCl_3$/C before (a) and after (b) the lignin gasification, $Ru(NO)(NO_3)_3$/C before (c) and after (d) the lignin gasification, and Ru/C before (e) and after (f) the lignin gasification. The closed and open circles indicate ruthenium metal and charcoal, respectively

catalysts (Fig. 1b). On the other hand, the percentage of methane on $RuCl_3$/C was lower.

Figure 2 shows XRD patterns of the $RuCl_3$/C, $Ru(NO)(NO_3)_3$/C, and Ru/C catalysts before and after the lignin gasification in supercritical water for 1 h at 673 K. Four XRD peaks at 38.8, 42.2, 44.4, and 58.4° for $RuCl_3$/C after the lignin gasification (Fig. 2b) are attributed to those for ruthenium metal and the broad peak around 43.6° is attributed to the charcoal support [17]. It was clear from the XRD pattern that the ruthenium metal species were formed in $RuCl_3$/C after the lignin gasification, indicating that ruthenium (III) was reduced to ruthenium metal during the lignin gasification in supercritical water; however, the metal particle size of the $RuCl_3$/C catalyst after the gasification could not be estimated using Scherrer formula because of poor peak separation. On the other hand, the peaks ascribed to ruthenium metal particles were not observed in the XRD pattern of Ru/C, indicating the high dispersion of ruthenium metal in the Ru/C catalyst. Inductive coupled plasma emission spectrometric analysis showed no ruthenium species were present in the liquid phase after the lignin gasification for any of the catalysts $RuCl_3$/C, $Ru(NO)(NO_3)_3$/C, and Ru/C, implying that all the ruthenium species existed on the charcoal support.

EXAFS spectra at Ru K-edge of the $RuCl_3$/C, $Ru(NO)(NO_3)_3$/C, and Ru/C catalysts after the lignin gasification in supercritical water for 1 h at 673 K were also studied. Figure 3 shows EXAFS oscillations and Fourier transforms of k^3-weighted EXAFS spectra for the ruthenium catalysts after the lignin gasification. The peaks of Ru–Ru were observed at 0.23 nm (phase shift uncorrected) in $RuCl_3$/C and $Ru(NO)(NO_3)_3$/C after the lignin gasification, indicating that ruthenium metal particles were formed in both ruthenium salt supported catalysts during the lignin gasification. The samples of catalyst suspension after the lignin gasification were transferred from the SUS reactors to the EXAFS cells immediately and measured under air-exposed conditions. Small amounts of ruthenium metal atoms of surface may be oxidized by air; however, Ru–O peaks were not observed in the Fourier transforms of EXAFS spectra (Fig. 3). One possible reason why Ru–O contributions were not observed is that ruthenium metal particles were not exposed to air directly because the samples were transferred to the EXAFS cells as water suspension and the metal particles were protected from oxygen in water. Table 2 shows structural parameters determined by a curve fitting analysis of the EXAFS Fourier transforms for the Ru/C, $RuCl_3$/C, and $Ru(NO)(NO_3)_3$/C catalysts after the lignin gasification along with the ruthenium metal powder as a reference sample. The Ru–Ru bond distance for the Ru/C, $RuCl_3$/C, and $Ru(NO)(NO_3)_3$/C catalysts corresponds with that of ruthenium metal, indicating the metal particle formation in all the samples. The *CN* of Ru–Ru bond for $RuCl_3$/C is 11.2 ± 2.3, confirming that large ruthenium metal particles were formed in $RuCl_3$/C, in accordance with the XRD result. On the other hand, the *CN* of $Ru(NO)(NO_3)_3$/C is 6.1 ± 1.2, which corresponds to the ruthenium metal cluster with number of atoms between 12 and 40 [18]. The size of ruthenium metal particle in $Ru(NO)(NO_3)_3$/C is equivalent to that of Ru/C within the margin of error of *CN* as shown in Table 2. Ketchie et al. reported that ruthenium metal particle on activated carbon were stable in aqueous phase using in-situ EXAFS technique [19]. They reported that the *CN* of Ru–Ru for Ru/C was 7.6 after the reduction by hydrogen at 473 K which slightly increased to 8.2 under 4 MPa hydrogen-saturated water at 473 K, demonstrating the stability of carbon-supported metal particles in water. In this work, we measured the EXAFS spectra of ruthenium catalysts using a rapid quenching method to elucidate the active site of ruthenium species for lignin gasification in supercritical water.

The ruthenium species in $Ru(NO)(NO_3)_3$/C was reduced to ruthenium metal particles, of which size was the same as that in Ru/C, and these two catalysts showed the same reaction time profiles for the lignin gasification as shown in Fig. 1a. These results can be explained reasonably well by a reaction mechanism involving the initial reduction of the $Ru(NO)(NO_3)_3$/C catalyst to ruthenium metal particles, which accelerated the lignin gasification leading to the same time profile as that for the Ru/C catalyst. We

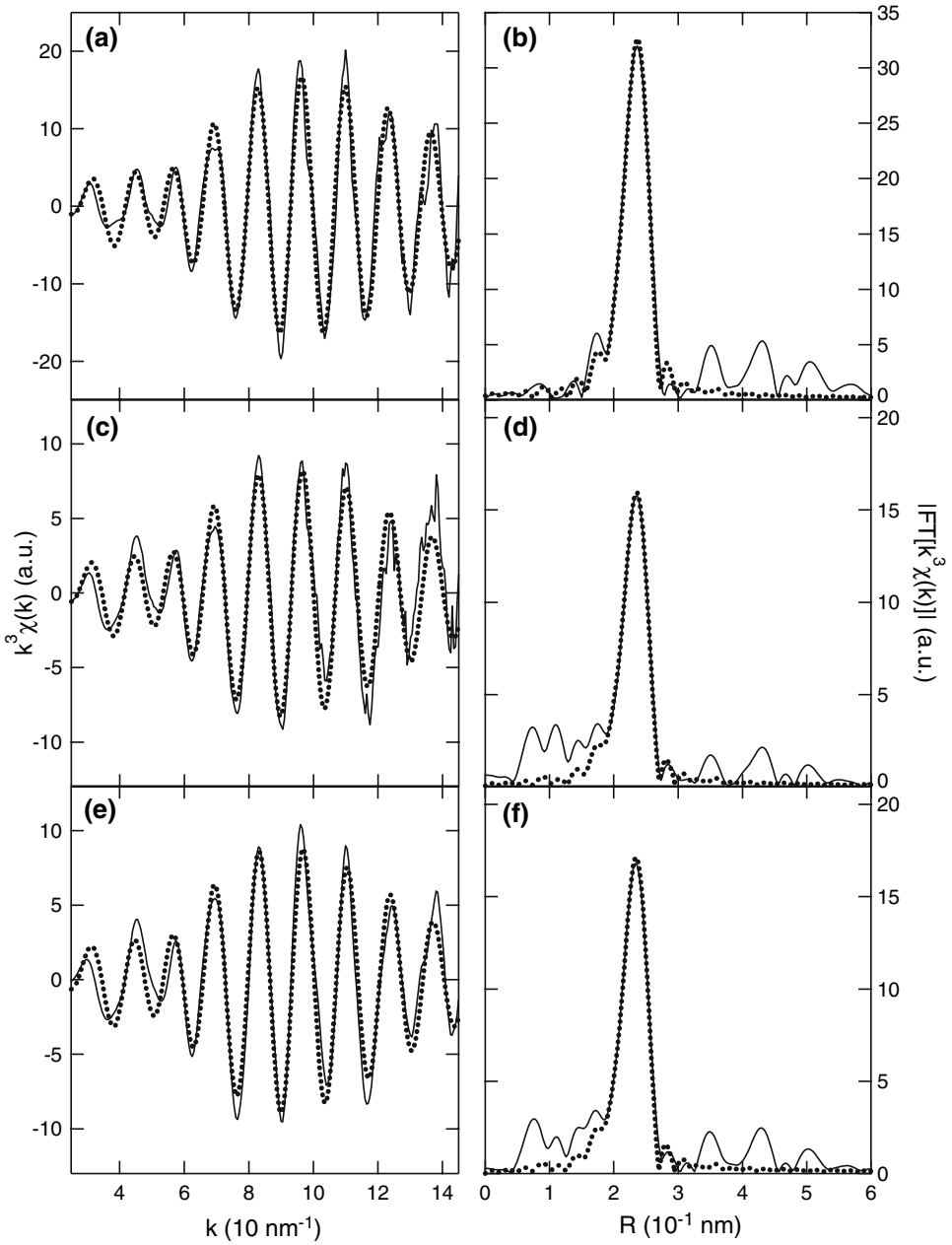

Fig. 3 EXAFS oscillations $k^3\chi(k)$ (**a**, **c**, **e**) and their Fourier transforms (**b**, **d**, **f**) for $RuCl_3$/C (**a**, **b**), $Ru(NO)(NO_3)_3$/C (**c**, **d**), and Ru/C (**e**, **f**) after the lignin gasification in supercritical water at 673 K for 1 h. Solid and dotted lines represent the experimental and the fitted results, respectively

Table 2 Structural parameters for Ru/C, $RuCl_3$/C, and $Ru(NO)(NO_3)_3$/C after the lignin gasification in supercritical water for 1 h at 673 K and Ru metal powder, determined by a curve fitting analysis of the EXAFS Fourier transforms

Sample	CN_{Ru-Ru}	R (nm)	σ^2 (10^{-5} nm^2)	ΔE_0 (eV)	R_f (%)
Ru metal powder	12.0[a]	0.267 ± 0.001	5.7 ± 0.5	−0.6 ± 2.9	2.5
$RuCl_3$/C	11.2 ± 2.3	0.267 ± 0.002	5.3 ± 0.2	−3.7 ± 5.1	1.0
$Ru(NO)(NO_3)_3$/C	6.1 ± 1.2	0.266 ± 0.002	6.5 ± 0.4	−5.1 ± 8.2	4.0
Ru/C	6.7 ± 1.1	0.266 ± 0.001	6.6 ± 0.8	−5.4 ± 1.8	2.3

[a] The coordination number was fix at 12.0

observed two complementary experimental results; (i) $Ru(NO)(NO_3)_3$/C was as active as the Ru/C catalyst for the gasification, while the $RuCl_3$/C catalyst was substantially less active than these catalysts, and that (ii) the size of ruthenium metal particles of the used $Ru(NO)(NO_3)_3$/C was as small as that of Ru/C catalyst, while the size of

metal particles of $RuCl_3$/C was bigger. These results led to the conclusion that the size of ruthenium metal particles, formed by the reduction of ruthenium trivalent salts during the lignin gasification in supercritical water, depends on ruthenium precursors and dramatically affects the gasification activity.

Lignin gasification occurs via two steps; (i) lignin decomposes to alkylphenols and formaldehyde via hydrolysis in supercritical water without a catalyst, and (ii) the gasification of alkylphenols and formaldehyde in the presence of supported ruthenium catalysts [9]. The latter step was catalyzed by ruthenium metal even in the case of un-reduced catalysts, $RuCl_3$/C and $Ru(NO)(NO_3)_3$/C. Lignin was almost completely gasified over $Ru(NO)(NO_3)_3$/C; however, lignin gasification over $RuCl_3$/C reached a plateau after 1 h (Fig. 1a). There are two possible reasons for the deactivation of the $RuCl_3$/C catalyst within 1 h. One is that large ruthenium metal particles were formed during the lignin gasification and the number of active metal sites was small in $RuCl_3$/C. Then, alkylphenols and formaldehyde from lignin reacted with each other again to form the char (THF-insoluble product). Another reason could be that chloride ions adsorbed on the ruthenium metal particles inhibited the gasification. We confirmed this possibility by the addition of hydrochloric acid, which decreased the gasification activity of Ru/C (gas yield, 30.2 C%; catalyst, 0.15 g; water density, 0.50 g cm^{-3}; temperature, 673 K; time, 1 h; moles of hydrochloric acid added was the same moles of chloride ion in $RuCl_3$/C). We did not observe the XRD peak ascribed to ruthenium metal particle in the Ru/C catalyst with hydrochloric acid (Fig. 4), indicating that chloride ions did not cause the enlargement of the size of ruthenium metal particles and inhibited the gasification.

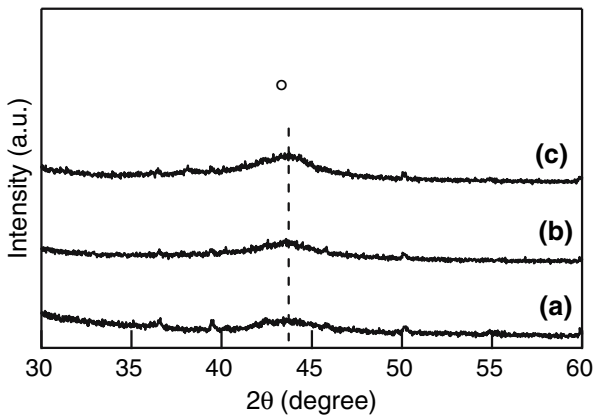

Fig. 4 XRD patterns for the Ru/C catalysts before (a) and after the lignin gasification in supercritical water at 673 K for 1 h in the absence (b) and presence (c) of hydrochloric acid. The open circles indicate charcoal support

Hence, both possibilities can cause the deactivation of $RuCl_3$/C.

We have reported that carbon monoxide and hydrogen were formed from lignin and that carbon dioxide and methane were produced via water–gas shift reaction and methanation reaction, respectively [7]. Water–gas shift reaction does not need ensembles of surface metal atoms, on the other hand, methanation reaction needs the ensembles of metal atoms [9]. We observed that the extent of methanation reaction over $RuCl_3$/C was also lower than those for $Ru(NO)(NO_3)_3$/C and Ru/C catalysts, similar to the activity pattern of lignin gasification. We also showed that the size of ruthenium metal particles for $RuCl_3$/C was larger than those for $Ru(NO)(NO_3)_3$/C and Ru/C, indicating that ensembles of surface metal sites in $RuCl_3$/C should be more than those in $Ru(NO)(NO_3)_3$/C and Ru/C. However, chloride ions act as a poison for the gasification, then actual ensembles and active sites in $RuCl_3$/C was much less than those in $Ru(NO)(NO_3)_3$/C and Ru/C. Thus, both the activity and selectivity to methane for $RuCl_3$/C were lower than those for $Ru(NO)(NO_3)_3$/C and Ru/C.

The lignin gasification involves the following steps, (i) lignin decomposition to alkylphenols and formaldehyde by supercritical water, (ii) gasification of alkylphenols and formaldehyde over ruthenium catalysts, and (iii) formation of char from formaldehyde. It was not possible to measure the rates of these individual steps, since the gasification was carried out in a batch reactor. We showed the overall gasification rates based on the initial gas yields and the weight of catalysts (Table 1). We confirmed that the gasification of 4-propylphenol proceeded over the $RuCl_3$/C and $Ru(NO)(NO_3)_3$/C catalysts with gas yield of 10 and 82 C%, respectively (4-propylphenol, 0.10 g; catalyst, 0.15 g; water density, 0.50 g cm^{-3}; temperature, 673 K; time, 1 h) and that ruthenium species underwent reduction to form metal particles during the 4-propylphenol gasification.

We also carried out blank experiments with the $RuCl_3$/C and $Ru(NO)(NO_3)_3$/C catalysts in supercritical water without lignin (catalyst, 0.15 g; water density, 0.50 g cm^{-3}; temperature, 673 K; time, 1 h) and observed the metal particle formation, as shown in Fig. 5 and Table 3. We found that the sizes of ruthenium metal particles formed in supercritical water without lignin were similar to those formed during the lignin gasification reaction. Therefore, we concluded that the un-reduced catalysts were reduced to ruthenium metal initially and then the active sites on the ruthenium metal surface catalyzed the gasification of alkylphenols and formaldehyde, which were produced from the lignin hydrolysis by supercritical water. The initial oxidation state of ruthenium species (ruthenium (III) or ruthenium metal) did not influence the lignin gasification

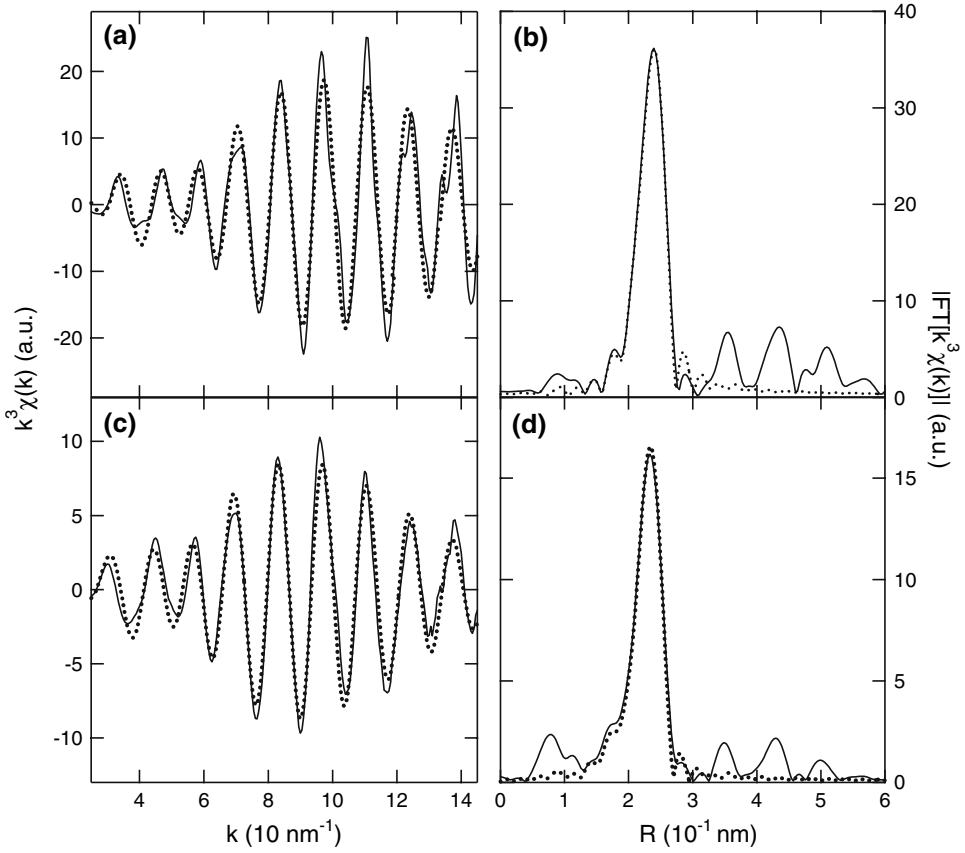

Fig. 5 EXAFS oscillations $k^3\chi(k)$ (**a**, **c**) and their Fourier transforms (**b**, **d**) for $RuCl_3$/C (**a**, **b**) and $Ru(NO)(NO_3)_3$/C (**c**, **d**) after the treatment in supercritical water without lignin at 673 K for 1 h. Solid and dotted lines circles represent the experimental and the fitted results, respectively

Table 3 Structural parameters for $RuCl_3$/C and $Ru(NO)(NO_3)_3$/C after the treatment in supercritical water without lignin at 673 K for 1 h, determined by a curve fitting analysis of the EXAFS Fourier transforms

Sample	CN_{Ru-Ru}	R (nm)	σ^2 (10^{-5} nm^2)	ΔE_0 (eV)	R_f (%)
$RuCl_3$/C	11.0 ± 1.1	0.267 ± 0.001	4.7 ± 0.4	3.0 ± 1.2	1.2
$Ru(NO)(NO_3)_3$/C	6.2 ± 0.6	0.265 ± 0.001	7.2 ± 0.4	−6.3 ± 0.9	1.3

activity directly, except indirectly through their effect on metal particle size.

3 Conclusions

Gasification of lignin in supercritical water at 673 K was studied over ruthenium trivalent catalysts ($RuCl_3$/C and $Ru(NO)(NO_3)_3$/C) and a charcoal supported ruthenium catalyst (Ru/C). The order of gasification activity was Ru/C ≈ $Ru(NO)(NO_3)_3$/C > $RuCl_3$/C. EXAFS analysis of the used supported ruthenium catalysts revealed that small ruthenium metal particles were formed during the lignin gasification in supercritical water and that ruthenium particle size in the $Ru(NO)(NO_3)_3$/C catalyst was smaller than that in the $RuCl_3$/C catalyst. It was concluded that supported ruthenium catalysts with the smaller size of metal particles were more active for the lignin gasification.

Acknowledgments EXAFS measurements were done by the approval of the PAC committee (proposal No: 2006G324).

References

1. Huber GW, Iborra S, Corma A (2006) Chem Rev 106:4044
2. Yoshida T, Matsumura Y (2001) Ind Eng Chem Res 40:5469
3. Watanabe M, Inomata H, Osada M, Sato T, Adschiri T, Arai K (2003) Fuel 82:545
4. Yoshida T, Oshima Y (2004) Ind Eng Chem Res 43:4097
5. Elliott DC, Sealock LJ, Baker EG (1993) Ind Eng Chem Res 32:1542
6. Davda RR, Shabaker JW, Huber GW, Cortright RD, Dumesic JA (2003) Appl Catal B 43:13
7. Osada M, Sato O, Watanabe M, Arai K, Shirai M (2006) Energy Fuels 20:930
8. Osada M, Sato T, Watanabe M, Shirai M, Arai K (2006) Combust Sci Tech 178:537

9. Osada M, Hiyoshi N, Sato O, Arai K, Shirai M (2007) Energy Fuels 21:1854
10. Park KC, Tomiyasu H (2003) Chem Commun 694
11. Izumizaki Y, Park KC, Tachibana Y, Tomiyasu H, Fujii Y (2005) Prog Nucl Energ 47:544
12. Osada M, Sato T, Watanabe M, Adschiri T, Arai K (2004) Energy Fuels 18:327
13. Wagner W, Prub A (2002) J Phys Chem Ref Data 31:387
14. Stern EA, Newville M, Ravel B, Yacoby Y, Haskel D (1995) Physica B 208:117
15. Ankudinov AL, Ravel B, Rehr JJ, Conradson SD (1998) Phys Rev B 58:7565
16. Osada M, Sato O, Arai K, Shirai M (2006) Energy Fuels 20:2337
17. Watanabe I, Sakanishi K, Mochida I (2002) Energy Fuels 16:18
18. Jentys A (1999) Phys Chem Chem Phys 1:4059
19. Ketchie WC, Maris EP, Davis RJ (2007) Chem Mater 19:3406